NEPHELOID LAYERS

I. N. McCave, University of Cambridge, Cambridge, UK

doi:10.1006/rwos.2001.0420

Introduction

A remarkable feature of the lower water column in most deep parts of the world ocean is a large increase in light scattering and attenuation conferred by the presence of increased amounts of particulate material. This part of the water column is termed the bottom nepheloid layer (BNL). The increase in light scattering is perceived relative to minimum values found at mid-water depths of 2000–4000 m (shallower on continental margins). The increased scattering is due to fine particles. This has been determined by size measurements and filtration of sea water with gravimetric analysis. Most data on the distribution and character of nepheloid layers have been gained by optical techniques, principally by the Lamont photographic nephelometer, the GEOSECS laser nephelometer, and the SeaTech transmissometer.

The optical work has revealed that the BNL is up to 2000 m thick (sometimes more in trenches) and generally has a basal uniform region, the bottom mixed nepheloid layer (BMNL), corresponding quite closely to the bottom mixed layer defined by uniform potential temperature (**Figure 1**). Above the BMNL there is a more or less exponential fall-off in intensity of light scattering up to the clear-water minimum marking the top of the BNL.

Another class of nepheloid layers found especially at continental margins comprise intermediate nepheloid layers (INL) (**Figures 1** and **2**). These occur frequently at high levels off the upper slope and at the depth of the shelf edge. From here they may spread out across the continental margin. These INLs are similar to the inversions observed in the BNL on some profiles (**Figure 1**).

The nepheloid layers of both types are principally produced by resuspension of the bottom sediments. Their distribution thus indicates the dispersal of resuspended sediment in the ocean basins. Most concentrated nepheloid layers occur on the continental shelf or deep continental margin. They give an indication of the locus of active resuspension and redeposition by strong bottom currents.

Optics of Nephelometers: What They 'See'

Most detection of deep-ocean nepheloid layers has been through measurement of light scattering. The Lamont nephelometer was used to make the largest number of profiles in all oceans but is no longer in use. It used an incandescent bulb as the source and photographic film as the detector of the light scattered from angles between $\theta = 8^\circ$ and 24° from the forward axis of the light beam. The film was continuously wound on as the instrument was lowered, resulting in an averaging of the received signal over about 25 m depth. The GEOSECS nephelometer used a red ($\lambda = 633$ nm) laser source and a photoelectric cell to detect light scattered from $\theta = 3^\circ$–15° off the axis of the beam. The SeaTech transmissometer, most commonly used now, has a red light source ($\lambda = 660$ or 670 nm) and usually a 0.25 m path length (1 m is also available).

Most of the contribution to the total scattering b comes from near forward angles (low values of θ). Jerlov showed that, for surface waters, 47% of b occurs between $\theta = 0^\circ$ and 3°, 79% between 0° and 15° and 90% between 0° and 30°. The GEOSECS instrument records about 32% of b and the Lamont nephelometer about 16%. The total scattering is given by Mie theory (assumed spherical particles) as a function of particle size d and relative refractive index n, and wavelength of light. The relative indices of refraction of suspended material are dominated by components with $n = 1.05$ and 1.15, values probably characteristic of organic and mineral matter respectively (e.g., RI of seawater 1.34, quartz 1.55, ratio 1.15).

Particles from clear ocean waters and weak nepheloid layers (concentration $C < 40$ mg m^{-3}) tend to have particle size distributions by volume which are flat, equivalent to $k = 3$ in a particle number distribution of Junge type, $N = Kd^{-k}$ where N is the cumulative number of particles larger than diameter d and K and k are constants. However, this distribution does not appear to be maintained at sizes finer than about 2 μm where k decreases towards 1.5. In concentrated nepheloid layers this distribution does not occur at all and a peaked distribution with a peak between 3 and 10 μm is encountered.

Morel has calculated scattering according to Mie theory for suspensions with Junge distributions and several indices of refraction. Recalculation into cumulative curves of percentage scattering in

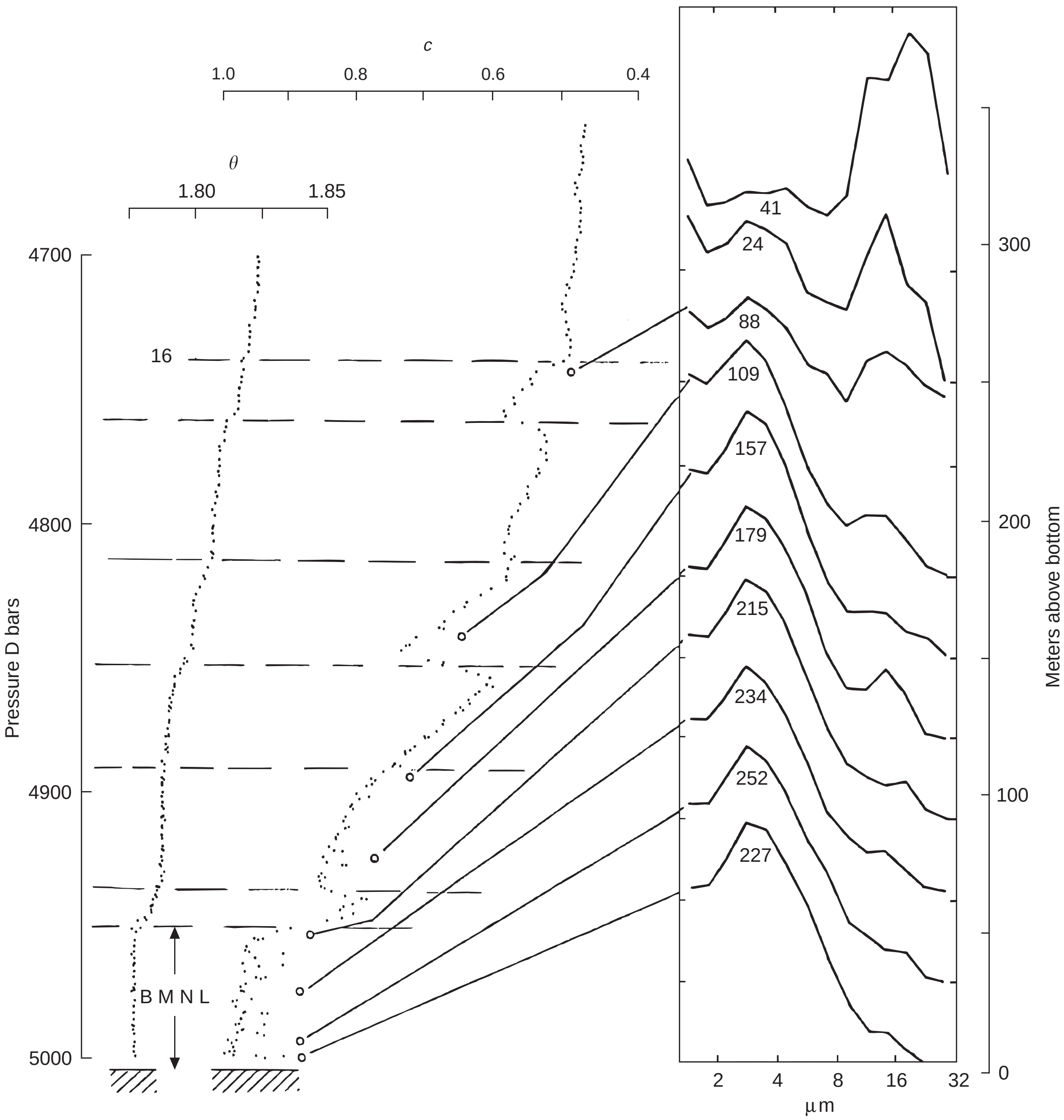

Figure 1 Data from the SeaTech transmissometer in the Atlantic showing the bottom-mixed nepheloid layer (BMNL) and a nepheloid layer comprising multiple steps in temperature and turbidity. Turbidity is given as c the attenuation coefficient, and potential temperature is θ°C. Also shown on the right are particle size spectra determined by Coulter counter. (Reproduced with permission from McCave, 1983.)

Figure 3 illustrates the fact that most recorded scattering is produced by fine particles. The cases shown are for values of k of 2.1, 3.2 and 4.0 and a two component (peaked) distribution with $k = 2.1$ up to $\alpha = \pi dn/\lambda = 32$ and $k = 4.0$ for larger sizes ($\alpha = 32$ is equivalent to $d = 5.6$ μm for $\lambda = 633$ nm). In each case three forward-scattering angles are given. It is clear that scattering close to the beam is more sensitive to large particles than that at 20°. (At $\theta < 0.5°$ we are essentially dealing with a transmissometer.) In the case of $k = 2.1$ only about 22% of the scattering is from smaller sizes ($\alpha < 32$) at $\theta = 20°$. Thus the curves for $\theta = 10°$ and 20° are generally representative, and the distribution for both $k = 3.2$ and the composite case show that 95% of the scattering is by particles < 5 μm for $\lambda = 633$ nm.

So it is dominantly the fine fraction of particles in nepheloid layers that is seen and recorded by nephelometers. These particles have very low settling velocities, less than 4.6×10^{-6} m s^{-1}. Although larger particles are present, they are rare and

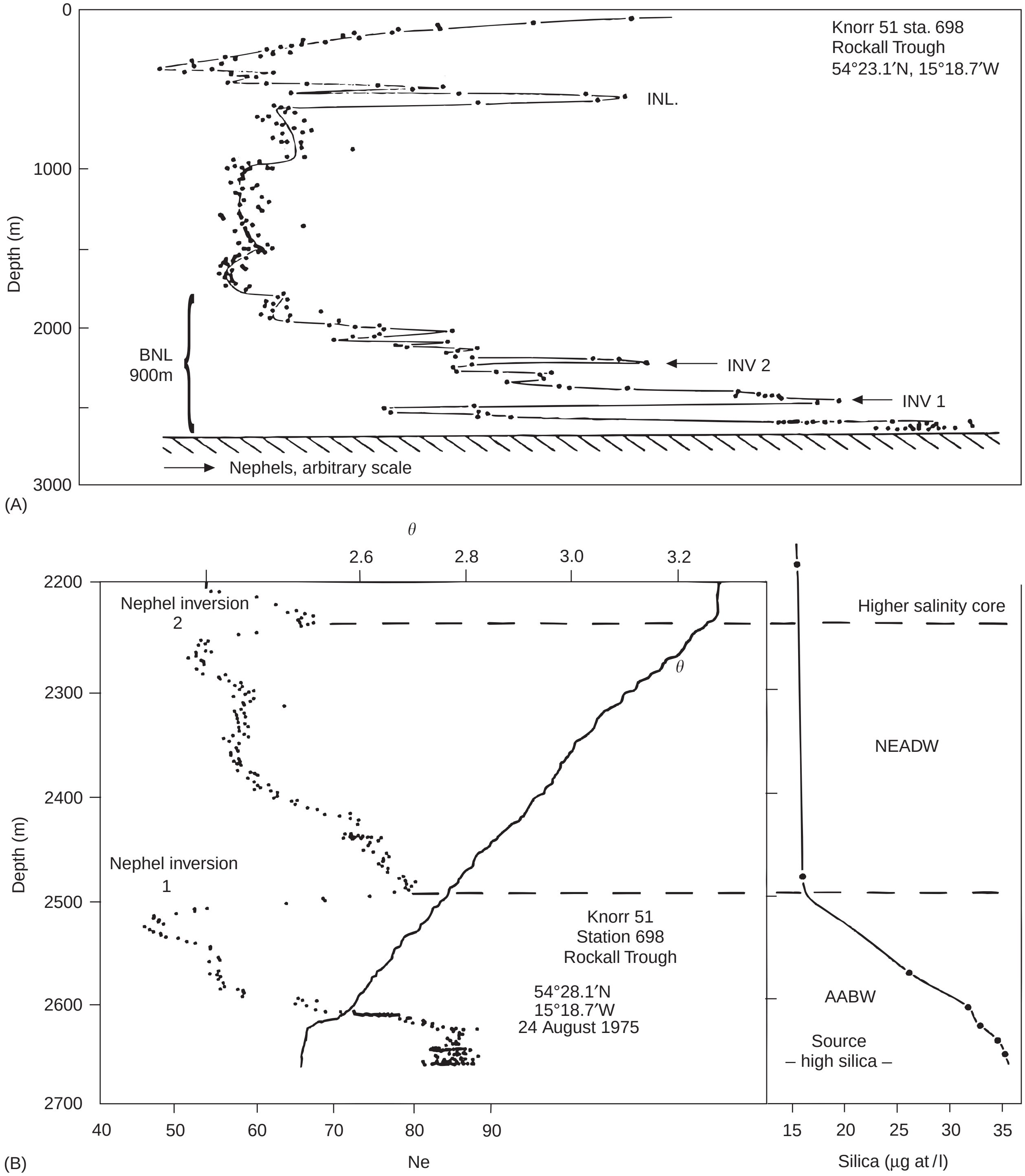

Figure 2 (A) Full-depth profile taken in the Rockall trough with the GEOSECS nephelometer. An intermediate nepheloid layer (INL) and two inversions are apparent. (B) Detail of the lower 500 m of the profile in (A) showing the relationship between the nephel (= turbidity) inversions and hydrography. (Reproduced with permission from McCave, 1986).

their properties and behavior cannot be invoked to explain features of distribution shown by nephelometers.

The SeaTech 0.25 m path length transmissometer has been used for most of the modern work on the structure and behavior of nepheloid layers. The transmission T is related to beam attenuation coefficient c over path length l as $T = e^{-cl}$. The major control of c is due to particles. Attenuation is due to absorption a and scattering b, thus $c = a + b$. The

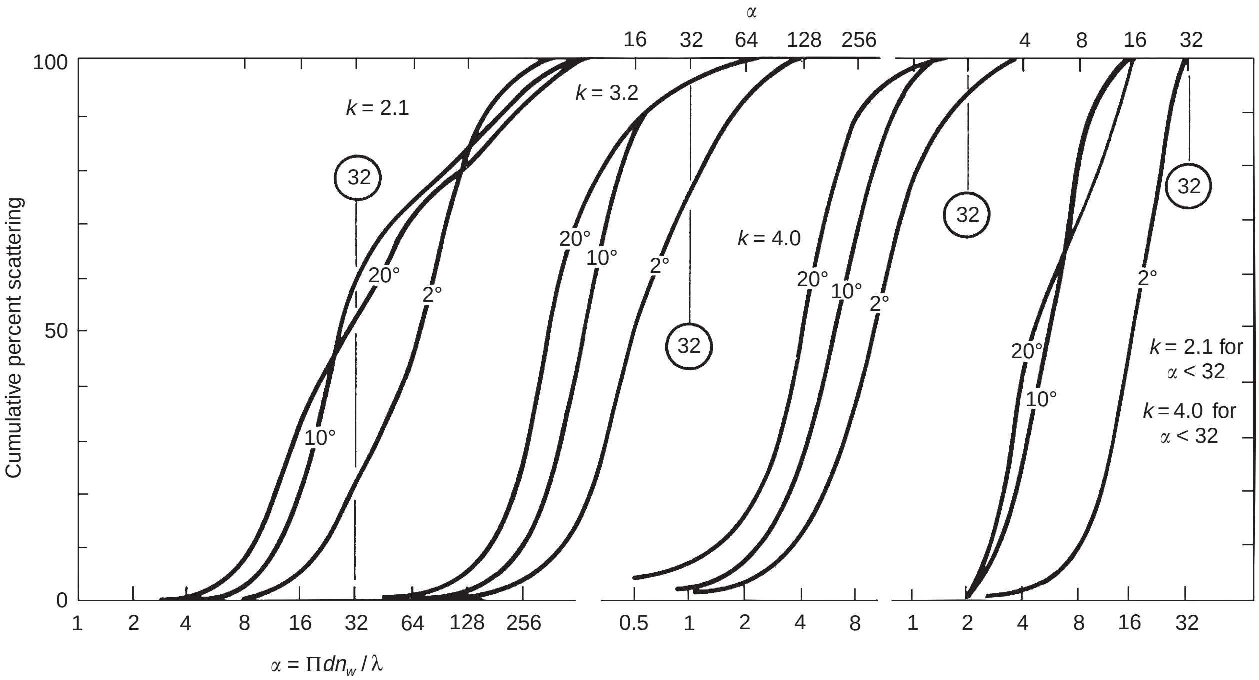

Figure 3 Cumulative percentage of scattering calculated from Morel's (1973) data by McCave (1986). The right-hand case is for a peaked distribution with the peak at $\alpha = 32$, equivalent to 5.6 μm for $\lambda = 633$ nm and $n = 1.15$. Note that material larger than the peak contributes virtually nothing to the scattering in this case. (Reproduced with permission from McCave, 1986.)

value of c for pure sea water is about 0.360 m^{-1} for this instrument operating at $\lambda = 660$ nm, and any excess is due to particulate effects. Because scattering very close to the beam is more sensitive to large particles, the transmissometer is more sensitive to larger particles and the nephelometer to smaller ones.

Nepheloid Layer Features

The principal features of nepheloid layers that must be accounted for are the facts that the concentration is generally highest close to the bed and decreases upwards. It is also important to note that this is not universally the case. Inversions, upward increases of concentration, are also found. Steeper gradients in the upward decrease of concentration as well as inversions are sometimes found at the boundaries of distinct density (temperature or salinity) changes. In the upper part of the bottom nepheloid layer such inversions become less common.

The thickness of the bottom nepheloid layer is generally in the region of 500–1500 m, and exceptionally up to 2000 m. This is clearly greater than the thickness of the bottom mixed layer (**Figure 1**), a fact which precludes the possibility of simple mixing by boundary turbulence being a sufficient mechanism for BNL generation.

In several cases the nepheloid layer is seen to transcend water masses. That is to say the nepheloid layer shows a general decline in turbidity upwards through interleaved water masses of differing sources and temperature/salinity characteristics. There may be a steeper turbidity gradient at the boundary between the water masses, but the nepheloid layer may continue through into the upper layer, usually without an increase in turbidity.

The highest turbidity appears to be in regions of strong bottom currents. Calibration of the nephelometer in terms of mass concentration of particulate material reveals that, in general, deep western boundary currents and regions of recirculation carry high particulate loads. However, the highest turbidity is also found beneath regions of high surface eddy kinetic energy (variance of current speed) located over strong thermohaline bottom currents. High surface eddy kinetic energy is connected with high bottom eddy kinetic energy, thus it seems likely that this motion, leading to intermittently very high current speeds when added to the strong steady component, may be responsible for intense sediment resuspension.

Separated Mixed-layer Model

Nepheloid layer structure is consistent with a vertical transport mechanism involving turbulent mixing in bottom layers of ~ 50 m thickness, followed by their detachment and lateral advection along isopycnal (equal density) surfaces. The detachment occurs where isopycnals intersect the bottom and this is likely to occur both in areas of steep topography with relief of hundreds of meters, and also in areas of lower gradient at benthic fronts where sloping isopycnals intersect the bottom. In many nepheloid layers there are sharp reversals, increases upwards, in nephel content associated with steps in other properties such as temperature and salinity. Both the step structure and inversions in particulate matter concentration are incompatible with turbulent mixing (which occurs only in the BMNL) up to a kilometer above the bed. It is not possible to mix sediment by turbulence across sharp density steps without breaking them down. However, these features are explicable if the layers are recently separated from the bottom. Some layers above the bottom mixed layer marked by steps in potential temperature contain excess radon-222 (originating from the bottom) with a 3.8 day half-life, suggesting detachment of bottom layers within the 2–3 weeks before sampling. It is anticipated that with time these layers thin by mixing at their boundaries and by lateral spreading to yield, eventually, a uniform stratification.

Decay of Concentration: Aging of Particulate Populations

The particles composing the nepheloid layer may be modified due to aggregation (*q.v.*) with similar sized particles and scavenging by larger rapidly settling ones (*q.v.* marine snow, trapped fluxes). Aggregation may also be caused through biological activity, although little is known about such processes at great depths. Particles tend to settle and to be deposited onto the bed, from the bottom mixed layer. The larger particles should be deposited in a few weeks to months, 10–20 μm particles taking 50–20 days to settle from a 60 m thick layer. This will not affect the layer perceived by nephelometers so quickly because the timescale of fine particle removal initially involves Brownian aggregation with a 'half-life' of several months to years.

The direct rate of deposition of very fine particles (0.5–1 μm) from a layer which remained in contact with the bed would be very slow. Concentration would halve in about 8 years. Thus the rate of decrease in concentration of 0.5–1 μm particles is due more to their being moved to another part of the size spectrum by aggregation than to their being deposited directly. The fine material in dilute nepheloid layers has a mean residence time measured in years. In more concentrated nepheloid layers a large proportion of this material will be removed in under a year. The dilute nepheloid layers in tranquil parts of the oceans could thus contain material that was resuspended very far away. The contribution of this material to the net sedimentation rate of these tranquil regions may not be negligible. The rate of deposition in the Pacific of only 0.5–2 mm ka^{-1} could include up to 1 mm ka^{-1} of fine material from the nepheloid layer.

With aging the individual detached layers comprising the nepheloid layer lose material by aggregation and settling and lose their identity by being thinned through shearing. An originally discontinuous vertical profile of concentration with inversions would be converted to one of relatively smooth upward decline in concentration. Present understanding of aggregation and sinking rates suggests that this takes a few years to achieve.

The Turbidity Minimum

The source of nepheloid layers at heights over a few hundred meters above the bed is believed to be the sides of the ocean basins and protrusions from the bottom of the oceans such as seamounts, ridges, and rises. Major source regions are deep zones of stronger currents, which in most areas are at depths greater than 3000 m, and shallow areas where material resuspended at the shelf edge and upper slope, possibly by internal wave motions in well stratified areas, spreads seaward. Tidal motion on the rough topography of mid-ocean ridges is known to yield enhanced mixing, and is also probably responsible for resuspension. Between these zones are depths of 1000–3000 m where stratification is weak, there are few zones of strong currents, there is no primary production of organic matter and the ocean is often undersaturated with respect to calcite, aragonite, and opal. There is thus a scarce supply from the side, and a decrease in downward transport due to dissolution and bacterial consumption of $CaCO_3$, SiO_2 and organic carbon leading to a nepheloid minimum where (in the Atlantic) concentrations are 5–20 mg m^{-3}. Below this the deep currents resuspend sediment on the continental margin and detached mixed layers are advected across adjacent abyssal plains. The upper part of the bottom nepheloid layer comprises sheared-out mixed layers that have, on average, come further from the sloping sides of the basins and from regions with less frequent resuspension, so they have lower concentrations. The basal part of layers is on average more recently resuspended and also gains material by fallout from above, thus there is an overall decreasing particulate concentration, and increasing age gradient upwards.

Concentration and Spreading in the Atlantic and Indian Oceans

The broad picture of high speed inflows on the western sides of ocean basins with a distributed return flow due to Stommel has been confirmed by many hydrographic studies and current measurements. These broad patterns of the inflow of cold bottom water are very similar to the excess BNL concentration (excess over the clear water minimum) for the Indian Ocean, and net BNL particulate load (mass per unit area) for the Atlantic based on Lamont nephelometer data (**Figures 4** and 5). It is also apparent that the concentration or load of sediment generally declines going northward along the paths of the major inflows of Antarctic bottom water.

However, there are several points of very high concentration or load which are not obviously related to likely increases in mean bottom flow velocity, for example, the high in the centre of the Argentine basin. These turbidity highs may be caused by intermittently high velocities under regions where high surface eddy kinetic energy was propagated downwards, resulting in high abyssal eddy kinetic energy. Some uncertainty remains over the role of high abyssal eddy kinetic energy versus locally accelerated thermohaline flow or deep recirculation loops in producing high concentration. Nevertheless, the major feature of concentrated bottom nepheloid layers is that they do delineate the

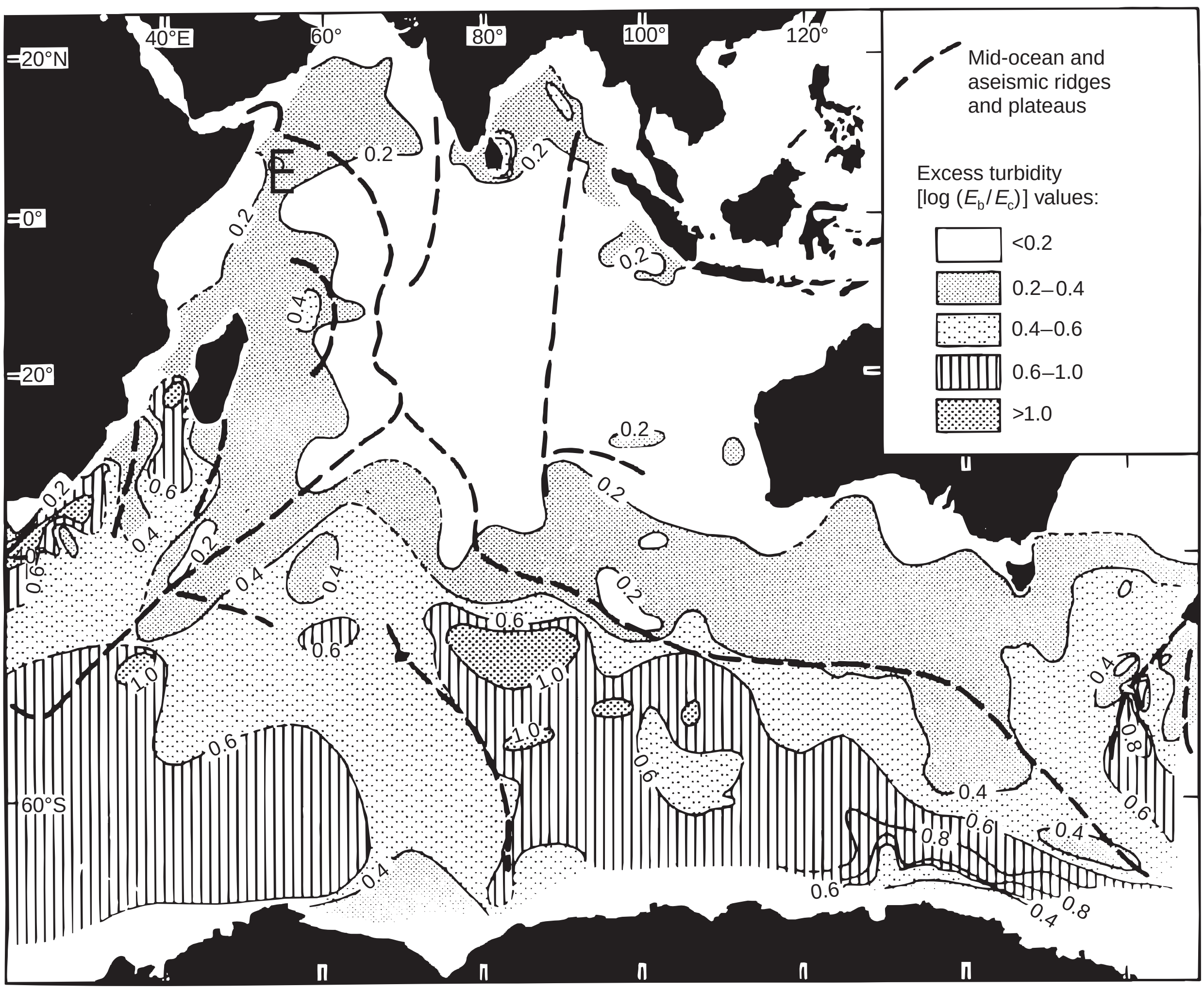

Figure 4 Distribution of excess turbidity for the Indian Ocean expressed as log(E/E_c) where E is the maximum light scattering near the bed and E_c is the value at the clear water minimum. A value of 1 thus represents a factor of 10 increase from the clear water value. Based on Lamont nephelometer data presented by Kolla *et al.* (1976, 1978). (Reproduced with permission from Kolla *et al.* 1976, 1978).

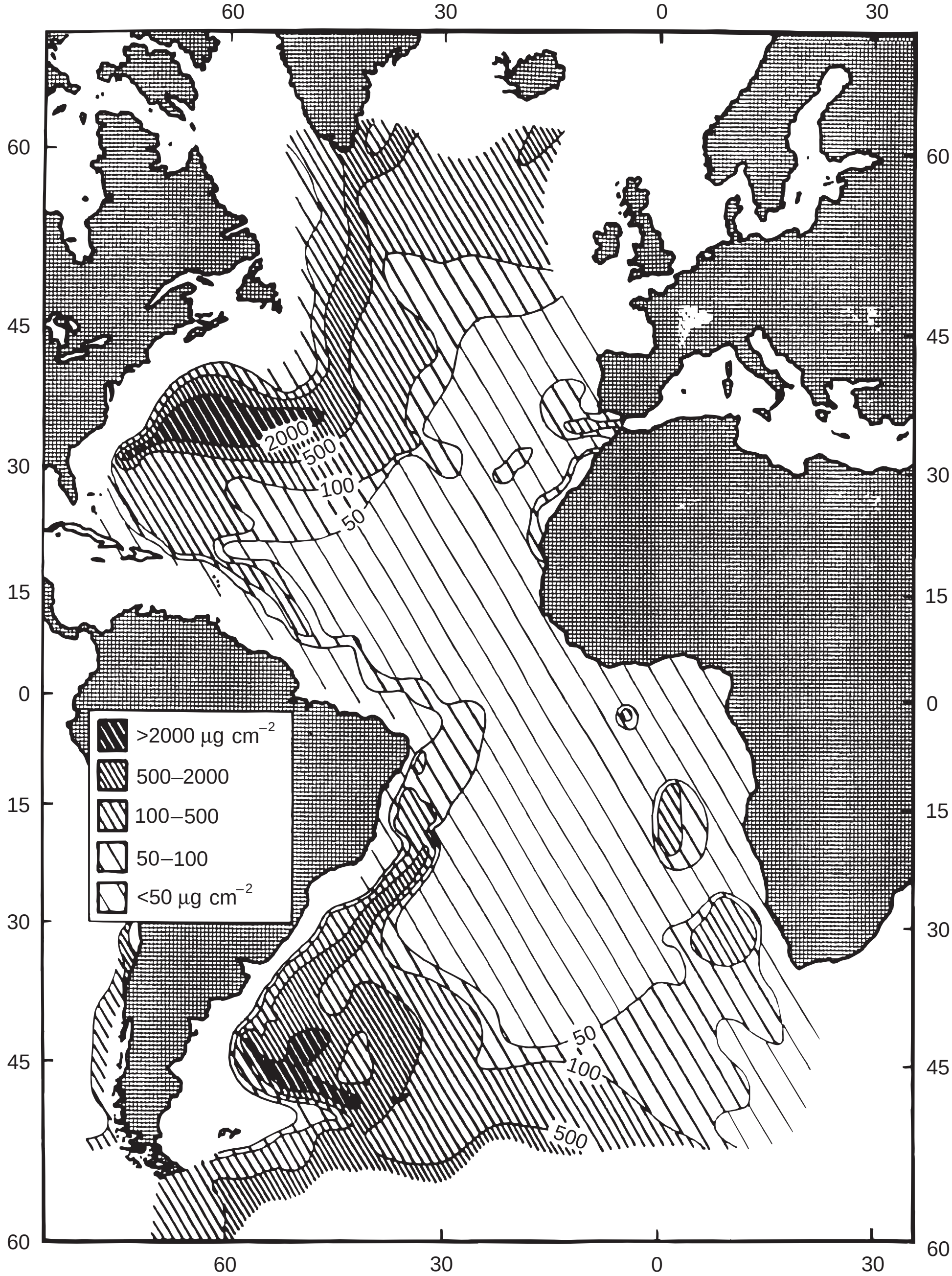

Figure 5 Distribution of excess suspended sediment load in the nepheloid layer. The load is computed for concentration excess over the value of the clear water minimum and integrated over the height of the nepheloid layer. (Reproduced with permission from Biscaye and Ettreim, 1977.)

paths of high velocity bottom currents extremely well and they decline in concentration away from high velocity boundary regions and away from the energetic Southern Ocean.

The concentrations given by nephelometers at the clear water minimum differ by a factor of about three between areas under high surface productivity (high) and mid-gyre regions (low). Thus, the flux of large particles from the surface in these areas appears to provide a net supply of smaller particles to mid-depth (rather than scavenging them). This is also seen to be the case in temporal variability at a point, such that higher mid-water turbidity occurs under higher summer productivity, and is lower in winter.

The transport in western boundary currents is very rapid. The tritium results of Jenkins and Rhines demonstrate a transit time of 15 years for Norwegian

Sea water from its source to the Blake Outer Ridge at 29°N, a distance of 6500 km. Given the long coagulation time of the particles composing nepheloid layers, a small fraction could have travelled from scour zones in the Denmark Strait overflow region. Thus nepheloid layers must be a complex mixture of particles of local and distant origins, which makes any attempt to trace their source through compositional analysis very difficult. It must always be remembered that the properties and behavior inferred from nephelometer data are biased towards small particles, but that larger particles are also present in the size spectrum.

Intermediate Nepheloid Layers, Inversions and Interflows

Although the presence of steps and inversions is best shown by modern high sampling-rate sensors (**Figures 1** and **2**), striking examples may also be found in older data. Pronounced inversions are seen at depths between 1 and 4 km along the continental margin close to the Congo (Zaire) River. A comparable situation is found over Nitinat Fan off the NW USA. This area lies off two submarine canyons which are the most likely sources of the intermediate layers. These layers may be produced by resuspension in canyons due to internal wave motions. Thus, canyons may also act as point sources for supply of turbid layers which mix out into the ocean interior. The best documented interflow is the turbid plume of the North Atlantic western boundary undercurrent, which leaves the bottom at the end of Caicos Drift at about 5200 m depth and proceeds at that level over the 8000 m deep Puerto Rico trench (**Figure 6**).

Trenches and Channels

A final example of the influence of the sides of a basin on the nepheloid layers in it comes from the extremely thick nepheloid layers found in trenches and some deep-sea passages. The nepheloid layer thickness is that of the trench depth plus the thickness of the nepheloid layer over the adjacent seafloor for the Kuril-Japan trench. The result is a layer 2600 m thick. Nepheloid layers 2700 m thick have been recorded in the Peru trench between 8° and 10°S (**Figure 7**). Flow through Vema Channel between the Argentine and Brazil basins yielded a water column well mixed in temperature and turbidity with excess radon-222 up to 400 m above the bed. Models of boundary layer development show that this cannot occur by vertical turbulent

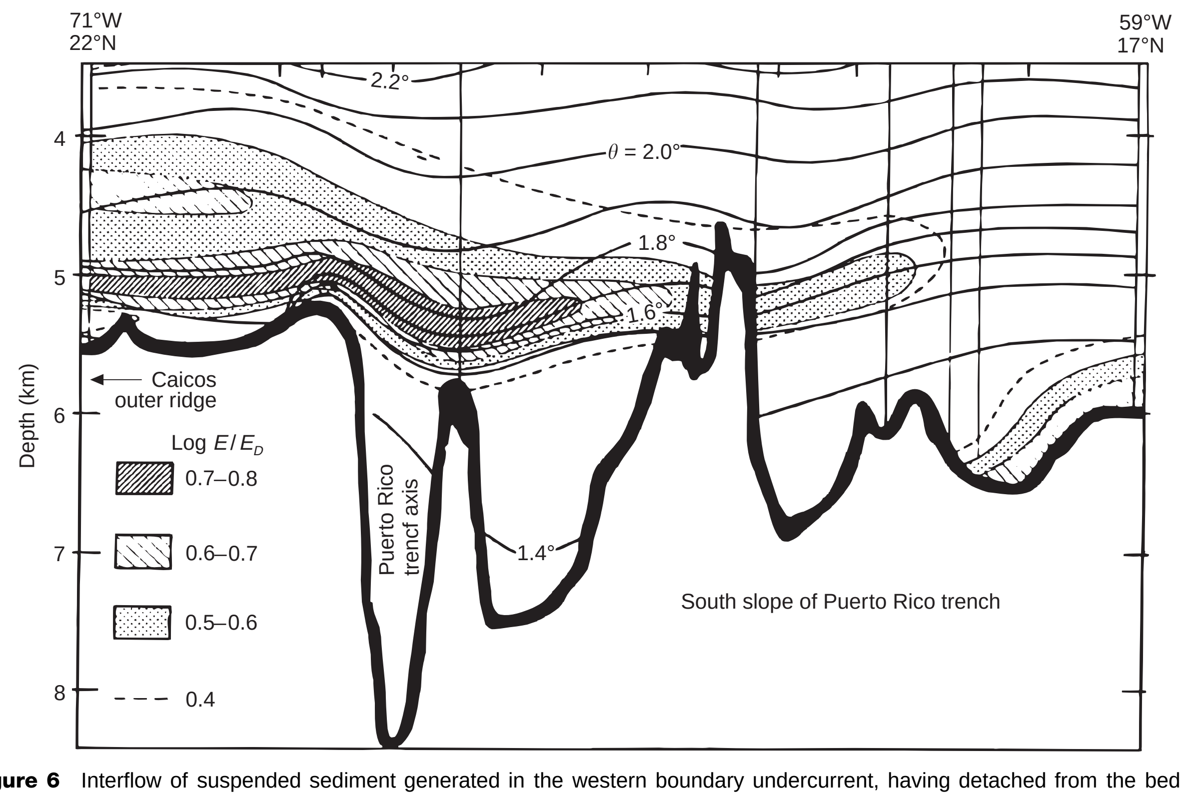

Figure 6 Interflow of suspended sediment generated in the western boundary undercurrent, having detached from the bed on Caicos drift, flowing over the Puerto Rico trench. (Reproduced with permission from Tucholke and Eittreim, 1974.)

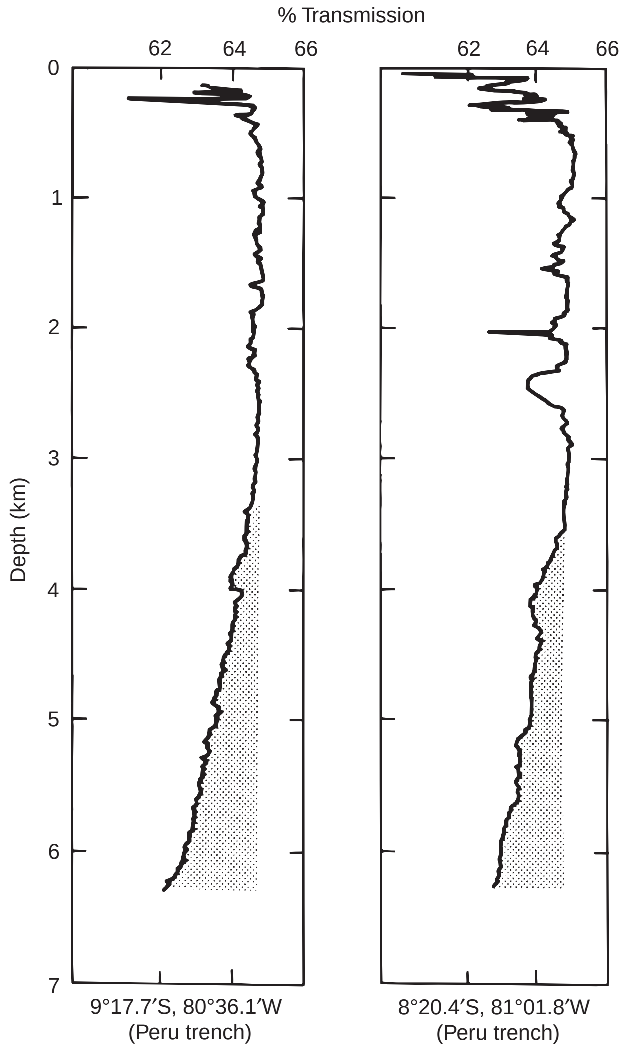

Figure 7 Profiles of the nepheloid layer in the Peru trench made with a 1 m path-length transmissometer. (Reproduced with permission from Pak *et al.* 1979.)

diffusion. Turbid layers must have migrated from the sides to the centre of the channel on a short timescale, giving added support to the detached mixed-layer model.

The fact that there is more suspended material at depths greater than about 4000 m partly reflects the fact that waters at those depths are in contact with a much greater area of sea bed in proportion to their volume than the shallower parts of the oceans. For 4–5 km depth the value is 0.83 km^2 km^3, whereas for 2–3 km it is 0.11 km^2 km^3. Deeper waters feel more bed. The global distribution of nepheloid layers is, for instrumental reasons, the global distribution of fine particles (< 2 μm) because that is what the instruments that map them 'see', but they also contain larger particles, especially in the lowest 10 m of the BMNL, which play an important role in particle dynamics.

See also

Marine Snow. Particle Aggregation Dynamics. Transmissometry and Nephelometry.

Further Reading

Armi L and D'Asaro E (1980) Flow structures of the benthic ocean. *Journal of Geophysical Research* 85: 469–484.

Bainbridge AE, Biscaye PE, Broecker WS et al. (1976) *GEOSECS Atlantic Bottom Hydrography, Radon and Suspended Particulate Atlas*. Scripps Institution of Oceanography: GEOSECS Operation Group.

Biscaye PE and Eittreim SL (1977) Suspended particulate loads and transports in the nepheloid layer or the abyssal Atlantic Ocean. *Marine Geology* 23: 155–172.

Dickson RR and McCave IN (1986) Nepheloid layers on the continental slope west of Porcupine Bank. *Deep Sea Research* 33: 791–818.

Gardner WD (1989) Periodic resuspension in Baltimore Canyon by focusing of internal waves. *Journal of Geophysical Research* 94: 18 185–18 194.

Jerlov NG (1976) *Marine Optics*. Amsterdam: Elsevier.

Jenkins WJ and Rhines PB (1980) Tritium in the deep North Atlantic Ocean. *Nature* 286: 877–880.

Johnson DA, McDowell SE, Sullivan LG and Biscaye PE (1976) Abyssal hydrography, nephelometry, currents and benthic boundary layer structure in Vema Channel. *Journal of Geophysical Research* 81: 5771–5786.

Kolla V, Sullivan L, Streeter SS and Langseth MG (1976) Spreading of Antarctic Bottom water and its effects on the floor of the Indian Ocean inferred from bottom water potential temperature, turbidity and sea-floor photography. *Marine Geology* 21: 171–189.

Kolla V, Henderson L, Sullivan L and Biscaye PE (1978) Recent sedimentation in the southeast Indian Ocean with special reference to the effects of Antarctic Bottom Water circulation. *Marine Geology* 27: 1–17.

Menard HW and Smith SM (1966) Hypsometry of ocean basin provinces. *Journal of Geophysical Research* 71: 4305–4325.

McCave IN (1983) Particulate size spectra, behavior and origin of nepheloid layers over the Nova Scotian Continental Rise. *Journal of Geophysical Research* 88: 7647–7666.

McCave IN (1986) Local and global aspects of the bottom nepheloid layers in the world ocean. *Netherlands Journal of Sea Research* 20: 167–181.

Morel A (1973) *Indicatrices de Diffusion Calculees par la Theorie de Mie pour les Systemes Polydisperses, en Vue de l'Application aux Particles Marines*. Lab.d'Oceanog. Phys., University of Paris VI, Report 10: 1–75.

Pak H, Menzies D and Zaneveld JRV (1979) *Optical and Hydrographical Observations off the Coast of Peru during May–June 1977*. Oregon State University, Corvallis, Data Report 77, Ref. 79-14: 1–93

Pond S and Pickard GL (1983) *Introductory Dynamical Oceanography*. Oxford: Pergamon.
Thomsen L and McCave IN (2000) Aggregation processes in the benthic boundary layer at the Celtic Sea continental margin. *Deep Sea Research I*, 47: 1389–1404.
Thorndike EM (1975) A deep sea, photographic nephelometer. *Ocean Engineering* 3: 1–15
Tucholke BE and Eittreim SL (1974) The western boundary undercurrent as a turbidity maximum over the Puerto Rico Trench. *Journal of Geophysical Research* 79: 4115–4118.
Zaneveld JRV, Roach DM and Pak H (1974) The determination of the index of refraction of oceanic particulates. *Journal of Geophysical Research* 79: 4091–4095.

NEPHELOMETRY

See **TRANSMISSOMETRY AND NEPHELOMETRY**

NETWORK ANALYSIS OF FOOD WEBS

J. H. Steele, Woods Hole Oceanographic Institution, Massachusetts, USA

doi:10.1006/rwos.2001.0291

Introduction

Photosynthesis transforms energy from sunlight into calories within marine plants, predominantly phytoplankton and seaweeds. The plants use this energy to take up carbon and essential nutrients, such as nitrogen and phosphorus, from sea water to produce organic materials. This organic matter forms the base for the food web composed of herbivores that eat those plants and the carnivores that prey on the herbivores. There can be several trophic levels of carnivores, including all the fish species that we harvest.

In the open sea, away from the coast and the seabed, microscopic single-celled phytoplankton dominate the plant life, so the organisms tend to get bigger as each trophic level feeds on the one below: from small herbivorous crustaceans to larger invertebrates, to small and large fish, and finally to human beings and marine mammals.

When any animal consumes food, most of the energy in that food is used for metabolism; some of the remainder is excreted as waste products and only a small fraction goes to growth. In young, cold-blooded animals in the sea, growth can be relatively efficient: 20–30% of energy intake. In older animals growth is replaced by reproduction, which, after all, is the whole point of the life cycle. As an approximate overall figure we usually assume that the energy converted into growth and reproduction is about 10% of the total energy intake. Thus, in a simple trophic pyramid, the energy in successive trophic levels would be 100:10:1:0.1. From this one can see why we are encouraged to eat plants on land, and why fish from the sea are energetically expensive in terms of plant calories.

In practice it is very difficult to measure directly the energy content of marine organisms and, especially the energy transfers between trophic levels. However, carbon is the essential building block for organic matter, being taken up from inorganic form at photosynthesis and returned to sea water during respiration. The carbon content of organisms and the rates of uptake of inorganic carbon can be measured using radioactive carbon, carbon-14, as a tracer; transfers through the food can then be measured. Carbon is therefore frequently used as a proxy for the more elusive concept of energy flow.

All organisms also require many essential elements, and many of these are in short supply in sea water. In particular, inorganic nitrogen and phosphorus, as nitrate and phosphate, are regarded as limiting factors in photosynthesis and thus in the rate at which energy and carbon are supplied to the food web. Since organic carbon, nitrogen and phosphorus have a roughly constant ratio in marine organisms (the Redfield ratio), nitrogen can also be used as a proxy for energy flow; it will not, however be considered here.

Carbon and nitrogen fluxes are also important in relation to other issues concerning marine food webs. The biologically mediated flux of carbon to deeper water is important for the calculation of global carbon budgets and climate change.